Shock Waves (2007) 17:215–223
DOI 10.1007/s00193-007-0108-8

ORIGINAL ARTICLE

Optical measurement and scaling of blasts from gram-range explosive charges

Michael J. Hargather · Gary S. Settles

Received: 14 May 2007 / Accepted: 10 September 2007 / Published online: 10 October 2007

Abstract Laboratory-scale experiments with gram-range explosive charges are presented. Optical shadowgraphy and high-speed digital imaging are used to measure the explosive-driven shock-wave position as a function of time. From this, shock Mach number-versus-distance from the explosion center can be found. These data then yield the peak overpressure and duration, which are the key parameters in determining the potential damage from an explosion as well as the TNT equivalent of the explosive. Piezoelectric pressure gage measurements of overpressure duration at various distances from the explosive charges compare well with theoretical calculations. A scaling analysis yields an approach to relate the gram-range blast to a large-scale blast from the same or different explosives. This approach is particularly suited to determining the properties and behavior of exotic explosives like triacetone triperoxide (TATP). Results agree with previous observations that the concept of a single TNT equivalence value is inadequate to fully describe an explosive yield, rather TNT equivalence factor and overpressure duration should be presented as functions of radius.

Keywords TNT equivalence · Blast waves · Gram explosive charges · Shadowgraph visualization

PACS 47.40.Nm

Communicated by B.W. Skews.

M. J. Hargather (✉) · G. S. Settles
Gas Dynamics Laboratory, Pennsylvania State University,
301D Reber Building, University Park, PA 16801, USA
e-mail: mjh340@psu.edu
URL: http://www.mne.psu.edu/PSGDL/

G. S. Settles
e-mail: gss2@psu.edu

1 Introduction

Explosive characterization is the process of quantifying explosive blast parameters relative to a standard. Typically TNT equivalence is reported, where explosion parameters or energy release are compared to the same results from an "equivalent" mass of TNT. This method is useful for estimation and comparative experiments, but it cannot describe the detailed differences in shock wave motion when different explosives are used [1]. Shock propagation speed determines the overpressure and its duration [2], thus explosives producing different shock speeds will have different overpressure and duration profiles. Such property differences result in different explosive impulses, damage potentials, and multiple "TNT equivalences" for the same blast [3] depending upon radius from the explosion center. To better characterize explosives, the shock wave radius and the overpressure duration as functions of time should be presented instead of mere TNT equivalence [4].

Shock wave propagation from large-scale blasts has been scientifically documented [5], but these tests are expensive and dangerous to researchers and test facilities. Recently, Kleine et al. performed explosive tests with 0.5–10 mg of silver azide and a laboratory-scale optical schlieren method [4]. These experiments pioneered the use and scaling of small explosive charges in economical and safe experiments. With the Hopkinson scaling law, mass, distance, and time can be scaled for explosives over a wide range of charge sizes [6]. Under the right circumstances, testing can be conducted at a laboratory scale and results extrapolated to large scale, reducing the need for full-scale tests.

The present research extends the small explosive charge characterization and scaling techniques pioneered by Kleine et al. [4] with milligram charges to the gram range. This research focuses on the measurement of shock wave

radius-versus-time using high-speed digital shadowgraphy. The experiments include the measurement of overpressure duration at various distances from the charge center. The collected data provide the basis for future gram-range-explosive materials testing.

2 Experimental procedure

2.1 Explosive charges

Two different explosives have been used in this research in order to document explosive parameter differences. The charge masses used here reflect ease of handling, manufacture, and safety considerations for each explosive material. An image of two typical charges is presented in Fig. 1.

Triacetone triperoxide (TATP), a primary explosive, was selected because of its recent use in terrorist activities [7]. The TATP was mixed with about 5% by mass nitrocellulose binder and formed into hemispheres. Two hemispheres were joined with liquid binder after placing a 0.15 mm tinned-copper wire through the center. The wire served as a hot-wire initiator for the primary explosive charge, powered by a 12 V automobile battery. Charge masses ranged from 0.5 to 4 grams. Each size was made in a hemispherical mold so that all charges were spherical.

Pentaerythritol tetranitrate (PETN) is a common and well-documented secondary explosive used in detonators for high explosives [8]. To initiate the PETN a 0.15 mm copper wire was used as an exploding bridgewire. Ground PETN crystals were mixed with 10% by mass nitrocellulose binder and pressed into cylindrical molds with the copper wire along the axis of the cylinder. The bridgewire initiation was driven by a commercial exploding-wire apparatus with 15 μF capacitance charged to 4,000 V. The methods for producing spherical TATP charges were unsuccessful when applied to PETN, but cylindrical charge molds worked well. Nominal PETN charge masses of 1 and 2 grams were used, with both molds having a length-to-diameter ratio of 1.

2.2 High-speed shadowgraph visualization

Each charge was detonated at the focus of a 0.76 m aperture, z-type optical focused shadowgraph system [9]. The focused shadowgraph technique allows the shock wave to be precisely imaged in the plane of the charge when the event is recorded with a high-speed digital camera. A 200 W Newport Xenon arc lamp provided continuous white-light illumination and a Photron APX-RS digital camera recorded the explosive event at frame rates from 10,000 to 250,000 frames per second with exposures of 1 μs per frame. A schematic of the shadowgraph system is given in Fig. 2. Theoretically, the shadowgraph effect should disappear when the camera is focused sharply on the explosive charge [9]. In this case, however, the shock wave of interest was strong enough and extended over a sufficient optical path length to provide well-defined shadows even when sharply focused.

Each test was recorded as a sequence of microsecond digital images of the shock wave propagating from the explosion center. Each sequence of images was then processed to locate and track the shock wave from the explosion center to the edge of the field of view. The position-versus-time history of the shock wave can then be used to determine shock Mach number and downstream properties throughout the event via the well-known Rankine-Hugoniot normal-shock theory. Shock position-versus-time data were extracted from the digital images using an image processing code written in MATLAB. A typical image sequence from an explosive test is shown in Fig. 3.

In order to check the symmetry of the shock waves produced from these small charges, a second shadowgraph system was set up perpendicular to the first, as shown in Fig. 4. The second system was an "Edgerton" retroreflective shadowgraph system [10]. This system used a 2 m retrore-

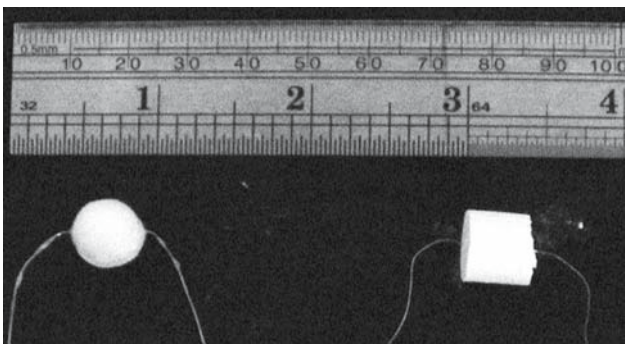

Fig. 1 1 gram TATP (*left*) and PETN (*right*) explosive charges. Both explosives are formed with a thin wire running through the center of the charge. The scale shows millimeters and inches

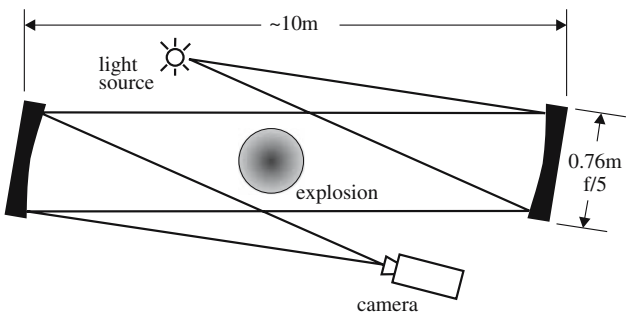

Fig. 2 The z-type focused shadowgraph system. The mirrors are 0.76 m aperture and the test section is roughly half way between the mirrors. The schematic is not drawn to scale

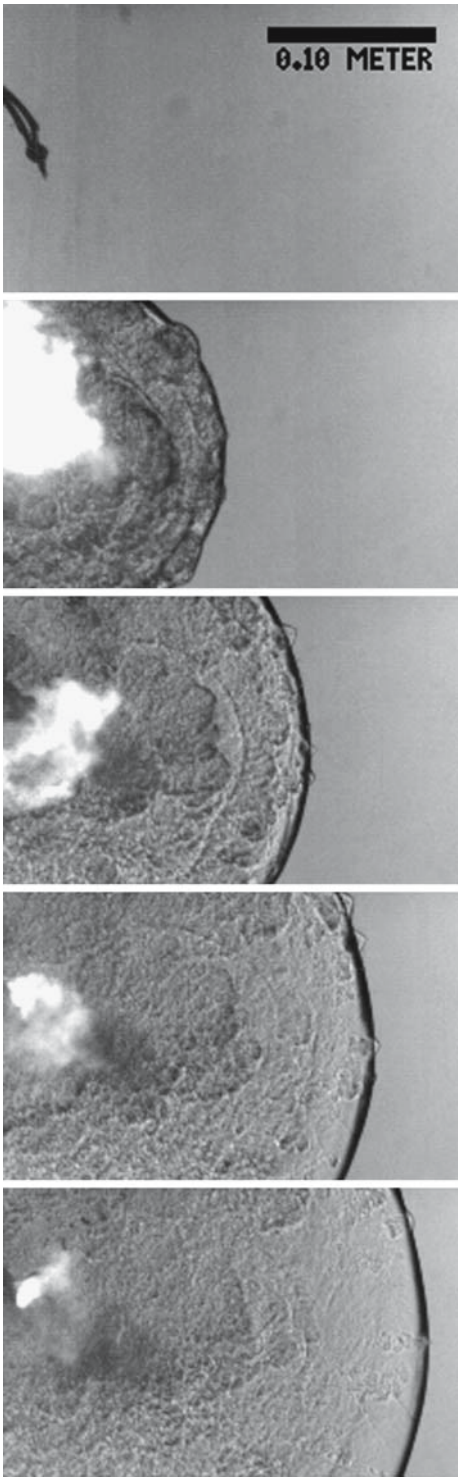

Fig. 3 Sample images from a test of 1 gram PETN, frames are 56μs apart

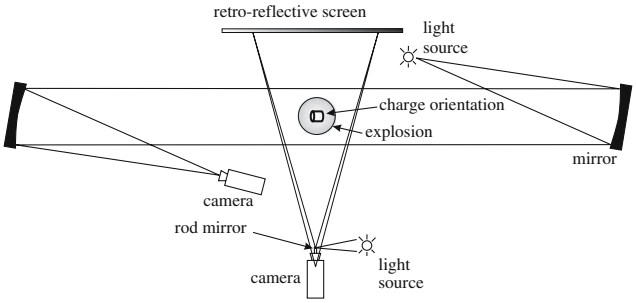

Fig. 4 A schematic of the perpendicular shadowgraph systems used to make simultaneous image sequences. The schematic is not drawn to scale

flective screen with a 1000 W Xenon arc lamp as an illumination source. A second Photron APX-RS digital camera, synchronized with the first, recorded the event at the same time as the master camera. The two systems together provided perpendicular views of the explosion, as shown in Fig. 5.

The focused shadowgraph images, shown on the left in Fig. 5, are sharper and show more detail, as expected. The retroreflective images, on the right in Fig. 5, are less sharp and not as detailed, though the shock front is still shown clearly. Images from the focused shadowgraph system are preferable because there is a one-to-one relationship between measurements in the image plane and the object plane when sharply focused. The retroreflective images require a simple geometric correction to relate the observed shock radius in the image plane to the actual shock radius, as shown by Dewey et al. [11].

When combined, the two views of the shock wave give an estimate of the degree of spherical symmetry. The 1 gram PETN charge was positioned so that the cylindrical axis aligned with the optical axis of the focused shadowgraph system. The resulting images from this system show a highly-symmetric shock wave at all distances from the charge. This is the plane of the shock wave that is measured both optically and with pressure gages. The second plane shown in Fig. 5 is the plane of the charge axis. The shock in this plane shows some asymmetry and residual shape due to the cylindrical shape of the charge. Huygen's Principle requires the eventual generation of spherical shocks, and within about 0.15 m of the charge center the irregular shock has become nearly spherical. This asymmetry is similar to that reported by Kleine et al. [4], but the present charges show better shock symmetry. This may be due to the more-symmetrical method of charge initiation.

The spherical TATP charges used here had no noticeable asymmetry when examined in the same manner.

2.3 Pressure measurement

PCB Piezotronics model 105C13 pressure gages and a model 481 signal conditioner were used to document the shock wave overpressure duration at various distances from the explosive charge center. The pressure gages were mounted and posi-

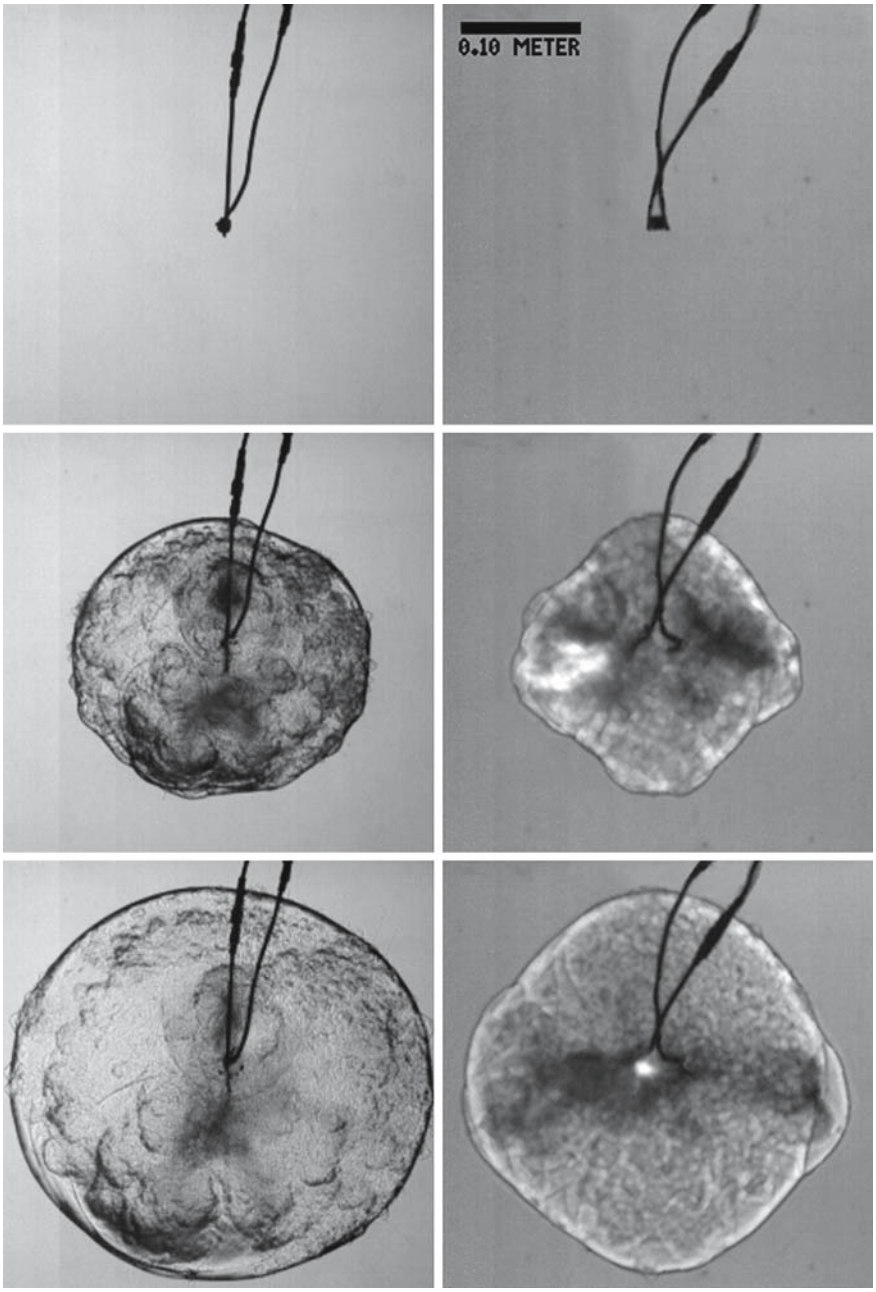

Fig. 5 Images from the simultaneous shadowgraph tests. The images from the z-type focused shadowgraph are on the left and the images from the retroreflective shadowgraph are on the right. The frames are 67μs apart

tioned face-on to the blast as described in Rahman et al. [12]. The positive pressure duration was measured and used to determine the positive impulse, the integral of pressure from the time of shock arrival to the end of the positive duration [13]. The negative impulse phase was ignored [6]. Gage inertia, response time, and noise make recording peak overpressure inaccurate, so the Rankine-Hugoniot relation was used to determine peak overpressure from the measured shock Mach number [2]. This is valid so long as the perfect gas assumption holds, which allows its use throughout the event except very close to the charge, where the high temperature behind the shock wave causes real-gas effects [14]. Thus no calibration for pressure is given in Fig. 6 because the peak overpressure is obtained by other means.

A typical unfiltered pressure trace recorded with the Tektronix TDS2000 digital oscilloscope and a 100 kHz low-pass-filtered signal are given in Fig. 6. The unfiltered data were noisy due to the small size of the charges and irregularities in the shock front. The filtered trace was used to determine the overpressure duration using the method outlined by Kinney and Graham [2]. The second peak in the pressure record was due to a shock reflection from the bracket holding the pressure gage. When determining the duration, only data points between the initial peak and this reflection were

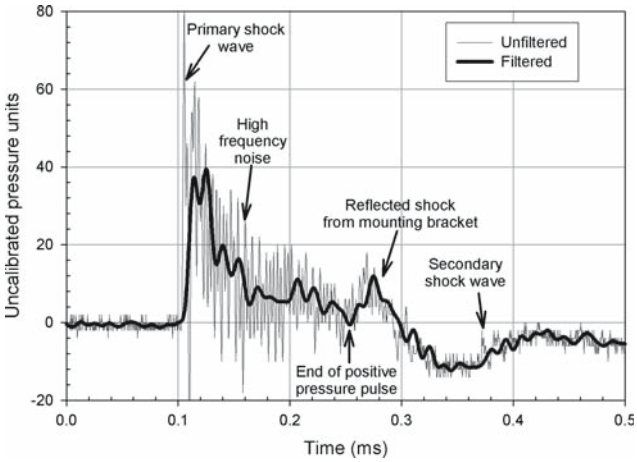

Fig. 6 Sample experimental pressure trace from the passing of a shock wave. The original and filtered data points are graphed. The duration is estimated by examining the exponential decay of the overpressure as described by Kinney and Graham [9]

used. The pressure rise from the secondary shock is insignificant compared to that from the primary shock. The location of the secondary shock was verified by comparing the time of arrival from the pressure trace with an image sequence showing the secondary shock passing the pressure gage.

3 Experimental results

3.1 Explosive scaling

Explosives are typically scaled using the Hopkinson or Sachs scaling laws. Hopkinson scaling assumes that similar shock waves are produced at scaled distances from two charges of the same material but with different masses, when detonated in the same atmosphere [6]. Sachs scaling accounts for temperature and pressure differences in the atmospheres in which charges are detonated [13]. Both scaling laws have been extensively confirmed on both large and small scales, e.g. by Dewey [5] and Kleine et al. [4], respectively. The scaling approach used by Kleine et al. [4] was also used here, where all experiments were scaled to Normal Temperature and Pressure (NTP). The scaling is given in Eqs. (1) and (2) and the scale factors are presented in Eqs. (3) and (4).

$$R_S = R/S \tag{1}$$

$$t_S = ct/S \tag{2}$$

$$S = (W/W_{std})^{1/3}(101.325/P)^{1/3} \tag{3}$$

$$c = (T/288.16)^{1/2} \tag{4}$$

Variables with subscripts S are the scaled values. R is the radius from the charge center, t is time, P is actual atmospheric pressure, T is actual atmospheric temperature, W is explosive mass, and W_{std} is the mass being scaled to, in this case 1 gram. Once scaled, the shock-wave-motion data points can be fit to Eq. (5) yielding coefficients A, B, C, and D, where a_0 is the speed of sound at NTP. For curvefits to data close to the charge center, B should be set to 1 to guarantee an asymptote to the speed of sound for large time [15]:

$$R_S = A + Ba_0t_S + C\ln(1 + a_0t_S) + D\sqrt{\ln(1 + a_0t_S)} \tag{5}$$

3.2 Shock tracking

To verify the scaling laws for TATP and PETN, charges of different masses were exploded and the shock wave radius versus time data were recorded with the shadowgraph system described above. Graphs of the measured and scaled data for TATP and PETN are given in Fig. 7. The measured data spread due to faster shock propagation with increasing charge mass. When scaled, the data collapse upon a single curve to within the error of the optical and image processing systems. Each set of data in Fig. 7 represents only a sample of the data recorded; multiple charges at each mass were exploded, revealing high repeatability between charges.

The scaled data for each explosive were combined from all tests and fit by least squares to Eq. (5), with B set to 1. The equation was then differentiated and manipulated to yield Mach number as a function of radius, the most important of present experimental results, which is given in Fig. 8. Also plotted in Fig. 8 are the "standard" values for 1 gram of TNT [2]. From this graph all post-shock gas property information can be generated using Rankine-Hugoniot or a real-gas theory.

The shock Mach number decays to 1 (a sound wave) within 0.5 m for these gram-range charges. Thus these charges are safe for indoor testing, where researchers require only hearing protection during a test when working several meters away, behind simple barricades. Limited data were obtained for $R \leq 0.03$ m because of camera speed resolution limits and the physical limit of the charge radius.

3.3 Pressure duration

The overpressure duration measurement completes the definition of explosive impulse for gram-range charges. Kinney and Graham [2] suggest that the duration can be calculated upon knowing the speed of the shock wave as a function of radius and assuming that the point marking the end of the positive pressure pulse (the "zero point") moves at the speed of sound based on gas temperature behind the shock wave. This "theoretical" duration can be calculated from the shock Mach number versus radius data by invoking the Rankine-Hugoniot theory. Each point in space is assumed to have a static temperature caused by a shock wave passing at a given Mach number. Simple gas dynamics calculations and a finite

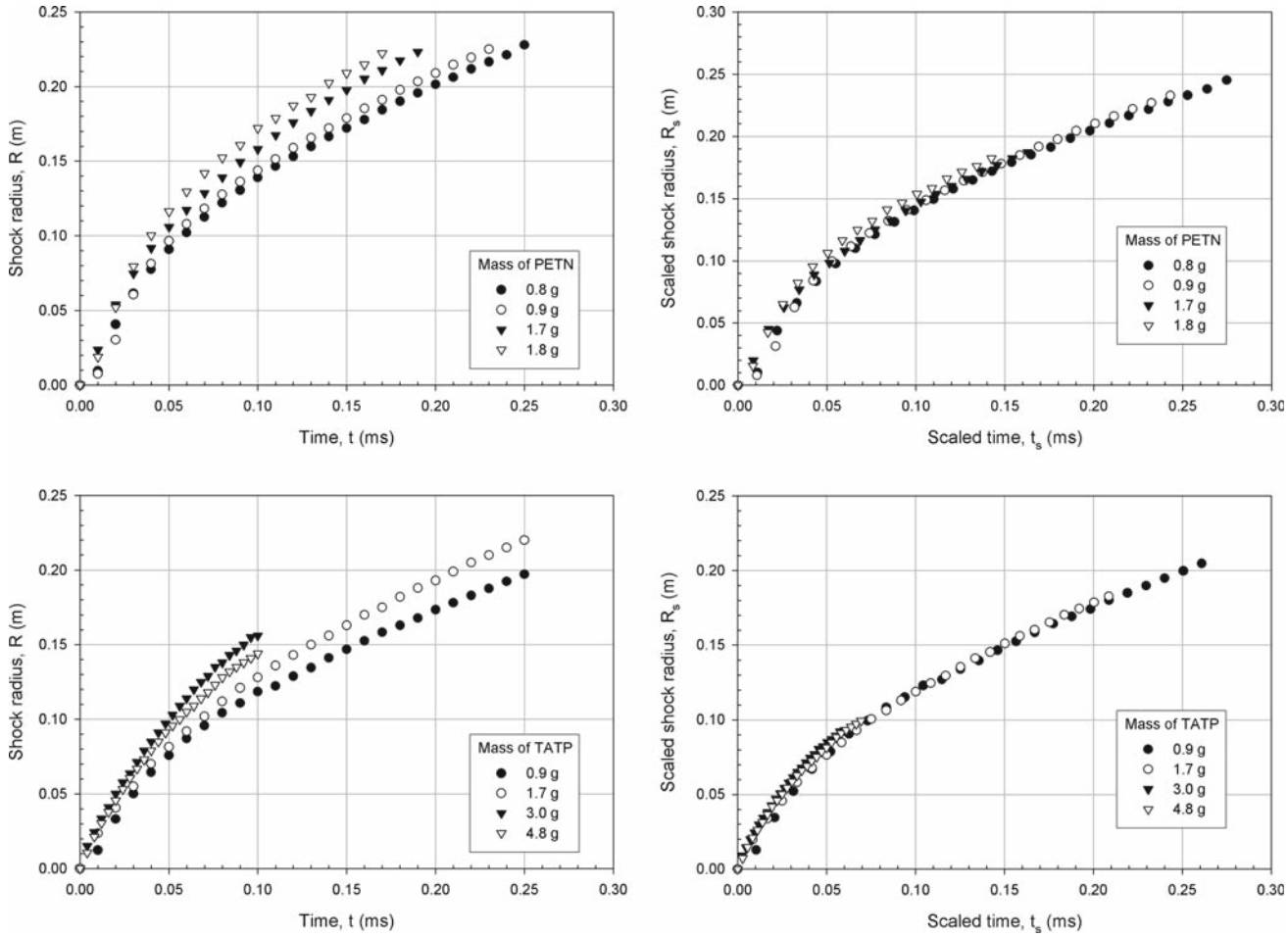

Fig. 7 Measured and scaled shock radius as a function of time for PETN and TATP. The scaled data is scaled to 1 gram charges. The error bar associated with each point is the size of the data point symbol, typically about 2 mm uncertainty in radius measurement. This represents a small sample of the total experimental data obtained

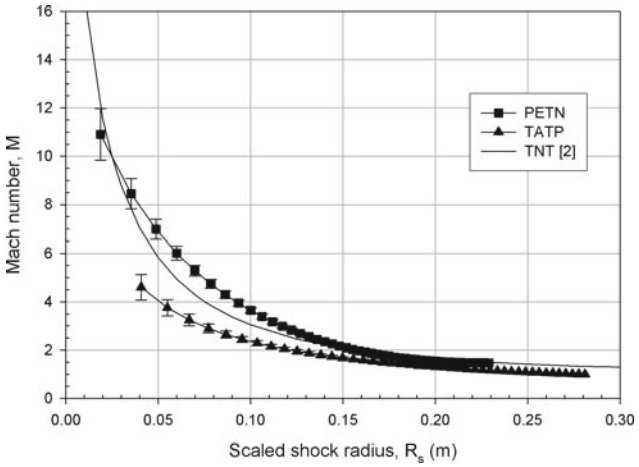

Fig. 8 Mach number as a function of scaled radius for 1 gram of PETN, TATP, and TNT. Error bars are shown for points where the error is larger than the curve marker symbol. Uncertainties for measurements when $R > 0.10$ m are typically about 3% of the Mach number

difference scheme can be used to propagate the shock front and zero point through space to estimate the overpressure duration.

Present experimental pressure duration measurements support Kinney and Graham's suggestion to within experimental error. More experiments should be performed, however, to further confirm this theoretical approach.

The predicted duration curves for TATP and PETN, calculated using the method above, along with experimental data for PETN, are given in Fig. 9. The experimental error varies inversely with radius due to possible irregularities in the shock front near the explosion center. The experimental and theoretical match shows the value of knowing the shock Mach number-versus-radius profile for an explosive, since it also determines the overpressure duration.

Explosive impulse, calculated from the peak overpressure and the overpressure duration, is a parameter that is used to scale damage to solid surfaces adjacent to a blast. While the

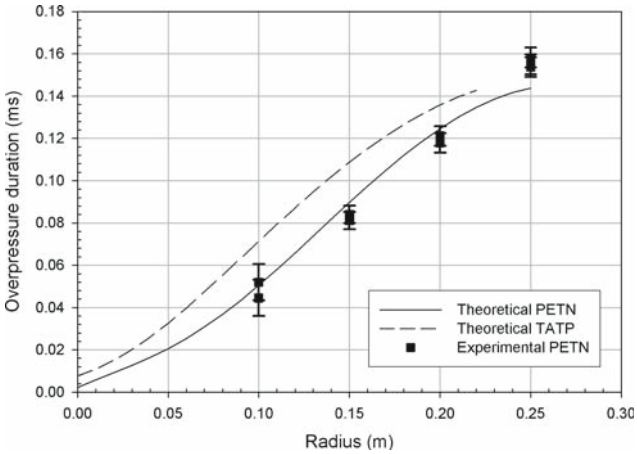

Fig. 9 Calculated and measured overpressure duration as a function of radius for PETN and TATP. Theoretical curves are determined using the method of Kinney and Graham [2]. The error in measured values decreases with increasing distance from the explosion center

present research is focused on understanding the explosive event, future work will address impulse effects on adjacent blast-resistant material samples.

3.4 TNT equivalence

One method of computing TNT equivalence is to find the mass of TNT required to cause the same overpressure at the same radius as a different mass of another explosive charge [4]. Thus the TNT standard shown in Fig. 8 is scaled by mass until the Mach number matches that of the desired explosive curve at each point. This process generates a variable TNT equivalence as a function of radius from the explosion center, as shown by Kleine et al. [4]. It is shown in Fig. 10 for TATP and PETN.

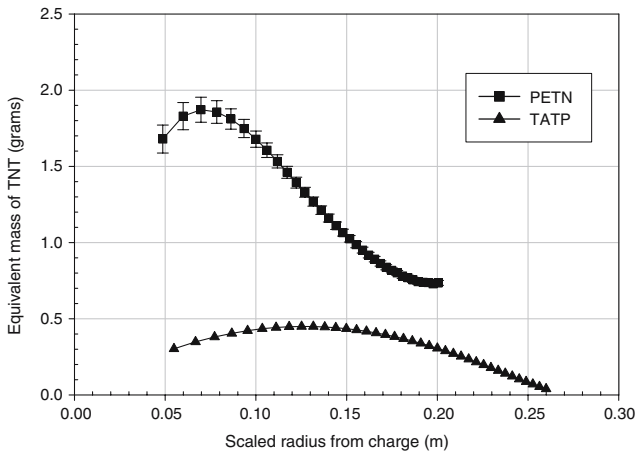

Fig. 10 TNT equivalence for 1 gram of PETN and TATP as functions of distance from the charge center

Previous TNT equivalence estimates for PETN range from 1.2 to 1.8 grams TNT per gram PETN depending on the type of test used to calculate equivalence [2]. The present research shows that the TNT equivalence actually varies between 0.7 and 1.8 depending on the radius from the explosion center. Similar results were published by Kleine et al. [4] for silver azide.

One published TNT equivalence value for TATP is 0.88 grams TNT per gram TATP [16]. The present data show a TNT equivalence range from 0.3 to 0.5 grams TNT per gram TATP. The TATP used here included a desensitizing polymer to stabilize the material, reduce volatility, and allow safer handling (Cho, I., personal communication). This could produce a lower TNT equivalence than pure TATP. However, the large discrepancy is more likely due to the different methods used to measure TNT equivalence here and in the work by Kemp [16]. The measurements shown here accurately represent the shock wave strength and the subsequent explosive damage potential.

These equivalence values based on the TNT "standard explosion" are expected to be valid over the majority of the shock wave radius range with the exception of its extremes. Both TNT equivalence curves show maximum values between scaled radii of 0.05 and 0.15 m. The decrease in equivalence at smaller radii is most likely due to significant errors near the explosion center. Limited camera resolution and other factors prevent more accurate measurements in this region. The high slope of the TNT Mach number-versus-radius curve in this region causes small errors in measured Mach number or radius to be magnified in determining TNT equivalence.

The decay of the equivalence curve with increasing radius is likely due to different chemical processes. TATP is a highly-non-ideal-explosive [17]. TNT is known to have an afterburning effect which changes the way in which the shock propagates, relative to an ideal explosion. Dewey has shown that TNT maintains a larger overpressure than an ideal explosion at large distances [13]. The difference in shock speed, and therefore TNT equivalence, is thus highly dependent upon the chemical mechanism by which the explosion process occurs. A detailed study of reaction mechanisms would be required to fully explain the TNT equivalence curve shapes of Fig. 10.

3.5 Experimental errors

Limited camera resolution caused some shock location tracking errors. Typically the shock location was determined to within two pixels. For each test a calibration image was taken to relate image pixels to a physical length in the image plane. Tests were conducted with different fields-of-view and camera speeds in order to optimize the data resolution. The most difficult measurements to make were near the explosion

center, where the largest error bars occurred. The repeatability of these experiments, over twenty trials, allowed a further reduction of the error bar size. Typical errors for all measurements with $R > 0.10\,\text{m}$ are on the order of $\pm 3\%$. Error estimates are presented on all figures either as explicit error bars or by the size of the data symbols.

Overpressure duration measurements have a wider error due to pressure-gage noise. The method for determining overpressure duration cited by Kinney and Graham [2] allows this error to be mitigated by examining a broad trend in the data. Measurements show good repeatability. The error bars are drawn based on two standard deviations. The error is about $\pm 5\%$ of the measurement level, with the largest error occurring nearest the explosion center.

4 Future work

The techniques used here should be applied to other explosives to build a library of explosive equivalent strength profiles. Larger-scale tests should also be performed to ensure the scalability of the results presented here.

More experiments should be performed to document the variation of overpressure duration as a function of radius, thus to further test the hypothetical variation proposed by Kinney and Graham.

The explosive characterization performed here can also be applied in future work on material blast response. The shock wave overpressure magnitude and duration profiles are the basis for this future work. With known Mach number-radius profiles, gram-range charges of different explosives and/or different masses can be exploded at various distances from a "witness plate" made of a known or candidate blast-resistant material. Ultimately, material response curves can be generated for a given overpressure magnitude, duration, or combined impulse. These response curves can be used to evaluate the blast mitigation properties of old and new shielding materials. Future materials testing will be challenged to scale material properties, but small-scale blast results will be useful for computational model validation and will provide better realism than typical drop-weight tests.

Gram-range explosive testing is not expected to entirely replace full-scale materials testing using charges at the kilogram level or larger. Nonetheless, gram-range testing has its applicability, the limits of which are yet to be determined.

5 Conclusions

A single TNT equivalence value is insufficient to define explosive strength parameters, as observed previously [4,18]. Shock wave Mach number and overpressure duration, as functions of radius from the explosion center, are required to properly define all parameters [4]. Here, TATP and PETN have been characterized by optically determining the shock wave radius-versus-time and by also measuring the overpressure duration as a function of radius. The pressure duration hypothesis of Kinney and Graham [2] was supported here for PETN, although more experiments should be performed for further validation.

This work also highlights the benefits of performing gram-scale experiments in the laboratory. These experiments are safer and cheaper than the equivalent full-scale tests. The optical methods and high speed digital imaging used in the laboratory environment allow more data to be recorded and more useful information to be derived than in typical full-scale outdoor explosive tests. These small-scale tests cannot fully replace full-scale tests, but they show useful potential. Inexpensive small-scale tests could be used to determine key experimental parameters and to bracket results to within an order of magnitude. Following gram-range testing, a limited set of full-scale tests should still be conducted to check the scaled results.

Acknowledgments This research was supported by the Transportation Security Laboratory, US Department of Homeland Security, via subcontract to the Battelle Corporation. The authors thank J. D. Miller, L. J. Dodson-Dreibelbis, H. Kleine, J. M. Dewey, J. A. Gatto, I. Cho, and D. J. Hernandez for their advice and support.

References

1. Held, M.: TNT-equivalent. Propellants Explosives Pyrotechnics **8**(5), 158–167 (1983)
2. Kinney, G.F., Graham, K.J.: Explosive Shocks in Air. Springer, New York (1985)
3. Cooper, P.W.: Comments on TNT equivalence. In: 20th International Pyrotechnics Seminar, pp. 215–226 (1994)
4. Kleine, H., Dewey, J.M., Ohashi, K., Mizukaki, T., Takayama, K.: Studies of the TNT equivalence of silver azide charges. Shock Waves **13**(2), 123–138 (2003)
5. Dewey, J.M.: Air velocity in blast waves from TNT explosions. Roy. Soc. — Proc. Ser. A **279**(1378), 366–385 (1964)
6. Baker, W.E.: Explosions in Air. University of Texas Press, Austin (1973)
7. McKay, G.J.: Forensic characteristics of organic peroxide explosives (TATP, DADP and HMTD). Kayaku Gakkaishi/J. Jpn. Explos. Soc. **63**(6), 323–329 (2002)
8. Cooper, P.W.: Explosives Engineering. Wiley-VCH, New York (1996)
9. Settles, G.S.: Schlieren and Shadowgraph Techniques: Visualizing Phenomena in Transparent media. Springer, Berlin (2001)
10. Settles, G.S., Grumstrup, T.P., Miller, J.D., Hargather, M.J., Dodson, L.J., Gatto, J.A.: Full-scale high-speed "Edgerton" retro-reflective shadowgraphy of explosions and gunshots. In: Fifth Pacific Symposium on Flow Visualisation and Image Processing (2005)
11. Dewey, J.M., McMillin, D.J.: High-speed photogrammetry of real and ideal reflections of spherical blast waves. J. Fluid Mech. **81**, 701–717 (1977)
12. Rahman, S., Timofeev, E., Kleine, H., Takayama, K.: On pressure measurements in blast wave flow fields generated by milligram charges. In: 26th International Symposium on Shock Waves (2007)

13. Dewey, J.M. : Expanding spherical shocks (blast waves). In: Ben-Dor, G., Igra, O., Elperin, E. (eds.) Handbook of Shock Waves, vol. 2, pp. 441–481. Academic Press, Boston (2001)
14. Anderson, J.D.: Hypersonic and High Temperature Gas Dynamics. McGraw-Hill, New York (1989)
15. Dewey, J.M.: In: Explosive flows: shock tubes and blast waves. Handbook of Flow Visualization, 1 edn., pp. 481–497. Hemisphere Publishing, Washington (1989)
16. Kemp, R.B., Brown, M.E., Gallagher, P.K.: Handbook of Thermal Analysis and Calorimetry, Applications to Inorganic and Miscellaneous Materials, vol. 2. Elsevier, Amsterdam (2003)
17. Dubnikova, F., et al.: Decomposition of triacetone triperoxide is an entropic explosion. J. Am. Chem. Soc. **127**(4), 1146–1159 (2005)
18. Dewey, J.M.: The TNT equivalence of an optimum propane-oxygen mixture. J. Phys. D: Appl. Phys. **38**, 4245–4251 (2005)